doi:10.4149/neo_2012_081

Novel nonclassical antifolate, 2-[*N*-(2′-Hydroxyethyl)amino]methyl-3*H*-quinazolin-4-one, with a potent antineoplastic activity toward leukemia cells

L. CIPAK

Cancer Research Institute, Slovak Academy of Sciences, Vlarska 7, 83391 Bratislava, Slovakia

Correspondence: exoncip@savba.sk

Received March 30, 2012 / Accepted May 18, 2012

This study was aimed to investigate the therapeutic potential of novel nonclassical antifolate, 2-[*N*-(2′-Hydroxyethyl)amino]methyl-3*H*-quinazolin-4-one (HEAMQ), toward human promonocytic U937 and murine lymphoblastic L1210 cell lines. The antiproliferative activity of HEAMQ was determined by MTT assay and its effects on cell cycle progression and apoptosis were studied by flow cytometry, and by immunoblots, respectively. In addition, combination chemotherapy of HEAMQ with cisplatin and temozolomide under *in vitro* and *in vivo* conditions was tested. HEAMQ showed concentration- and time-dependent cytotoxicity toward U937 and L1210 cells. It induced G_2/M arrest that in U937 cells was associated with a marked decrease in the protein expressions of cyclin A, cyclin B, and cyclin-dependent kinase Cdk1. HEAMQ-induced apoptosis was accompanied with up-regulation of the protein expression of Bax and down-regulation of the protein expression of Bcl-2, Mcl-1, XIAP, and survivin, resulting in cytochrome *c* release and activation of caspases. Inhibitors of JNK (SP600125) and p38 MAPK (SB203580) suppressed HEAMQ-induced apoptosis and G_2/M phase arrest, attenuated the activation of Bax, and blocked down-regulation of Bcl-2, XIAP and survivin in HEAMQ-treated U937 cells. In addition, combinations of HEAMQ with cisplatin and temozolomide resulted in synergistic inhibition of cell growth, producing long-term survivors of L1210 tumor-bearing mice. In conclusion, these results indicate that HEAMQ antineoplastic activity toward leukemia cells is associated with cell cycle arrest and apoptosis. The *in vivo* studies further confirmed the antitumor activity of HEAMQ and highlighted that this agent could be used to further increase therapeutic efficacies of traditional chemotherapeutic agents.

Key words: nonclassical antifolate, quinazolinone, antineoplastic, apoptosis, cell cycle arrest, synergism

Cancer is a serious disease with a complex pathogenesis. A number of chemotherapeutic drugs have been developed to treat cancer. These drugs exert their antiproliferative and DNA damaging activities by disturbing the cell cycle progression and by induction of apoptosis [1]. Cell cycle progression is regulated by the coordinated action of cyclin-dependent protein kinases in association with specific regulatory cyclin proteins. Activation of the complex of Cdk1, Cdk2 with cyclin A and cyclin B is essential for transition of cells from G_2 to the M phase of the cell cycle [2]. Activation of caspases is regulated by various cellular proteins including members of the inhibitor of apoptosis (IAP) or Bcl-2 families [3,4]. Previous studies have demonstrated that some Bcl-2 family members (Bax, Bcl-X_L, Mcl-1, Bid and Bcl-2) that are located on the mitochondrial membrane can alter its permeability and trigger the activation of caspases leading to apoptosis [5]. The mitogen-activated protein kinase (MAPK) superfamily is important mediator of apoptosis induced by stress stimuli. JNK and p38 MAPK pathways are activated in response to chemicals and environmental stress, while the ERK cascade, activated by mitogenic stimuli, is critical for proliferation and survival [6,7]. Recent evidence indicates that JNK signaling pathway affect the members of the Bcl-2 family. JNK can act as an activator in eliciting mitochondrial translocation of Bax [8]. Activation of p38 MAPK distorted mitochondrial function via an increase in the ratio of Bax and anti-apoptotic members leading to an increase in mitochondrial membrane permeability, the release of cytochrome *c*, and activation of caspases [9].

Quinazolinone is a naturally occurring alkaloid found in a variety of bioactive natural products and possesses wide range of biological activities. Its derivatives have found attractive applications as pharmaceutics. They are used as antibacterial, antimalarial, antileishmanial, antituberculosis, antiinflammatory, antirheumatic, antiulcer, anticonvulsant or cardiac

stimulant agents [10,11]. It has been showed that they possess potent cytotoxic and antitumor activities by inhibiting of P-glycoprotein, topoisomerases I and II, PDGF receptor tyrosine kinase or PI3-kinase-related kinases (PIKKs). Some quinazolinones induce cell cycle arrest, generate reactive oxygen species, disrupt mitochondrial membrane potential, induce single-strand DNA breaks and activate caspases [10-14].

In continuation to our effort on the design of potent anticancer agents, novel quinazolinone-based nonclassical antifolates were prepared and their antiproliferative potential was assessed [15]. In our pilot study, we found that many of these compounds exhibited potent cytotoxicity against leukemia cells. Among them, 2-[*N*-(2′-Hydroxyethyl)amino]methyl-3*H*-quinazolin-4-one (HEAMQ) was found to be the most potent compound toward leukemia cells, with activity comparable to that of methotrexate, with IC_{50} value in nM range [16]. Additionally, HEAMQ proved to be multi-targeted agent active toward various cancer cell lines (e.g. HL-60, U937, L1210, A549, Capan-1, HCC1837).

In this study, we report that antineoplastic activity of HEAMQ toward U937 and L1210 leukemia cells is associated with G_2/M cell cycle arrest, down-regulation of cyclin-dependent protein kinases, dysregulation of Bcl-2 family members and induction of apoptosis in leukemia cells. Importantly, we found that combinations of HEAMQ with traditional chemotherapeutic agents resulted in synergistic inhibition of leukemia cell growth *in vitro* and *in vivo*.

Materials and methods

Chemicals. 2-[*N*-(2′-Hydroxyethyl)amino]methyl-3*H*-quinazolin-4-one (HEAMQ) was prepared as described previously [15]. Chromatographically pure HEAMQ was dissolved in 100% DMSO. Final concentration of DMSO never exceeded 0.05% (v/v) in either control or treated cells. RPMI 1640 medium, fetal calf serum (FCS), phosphate buffer saline (PBS), L-glutamine, penicillin and streptomycin were obtained from Biocom (Slovakia). 3-(4,5-Dimethylthiazol-2-yl)-2,5-diphenyltetrazolium bromide (MTT), DMSO, ribonuclease A (RNAse), propidium iodide (PI), SB203580, SP600125, PD98059, cisplatin and temozolomide were purchased from Sigma-Aldrich (St Louis, MO, USA). Primary and HRP-conjugated secondary antibodies were obtained from Santa Cruz Biotechnology (Santa Cruz, CA, USA). PVDF membrane was purchased from Bio-Rad Laboratories Ltd. (Bio-Rad, CA, USA), Pierce® ECL Western Blotting Substrate was obtained from Thermo Fisher Scientific (Thermo Scientific, IL, USA) and Protease inhibitor cocktail tablets were purchased from Roche Applied Science (Roche Diagnostics GmbH, Vienna, Austria). The colorigenic synthetic peptide substrates, Ac-DEVD-pNA and Ac-LEHD-pNA were obtained from Calbiochem (La Jolla, CA, USA).

Cells. The human promonocytic U937 and murine L1210 lymphoblastic cell lines, obtained from the ATCC (Rockville, MD, USA), were cultured in RPMI 1640 medium supplemented with penicillin (100 U/ml), streptomycin (100 μg/ml), L-glutamine (292.3 μg/ml) and 10% heat-inactivated FCS in an atmosphere of 5% CO_2 in humidified air at 37°C.

Cell viability assay. Cell viability was assayed using a MTT assay [17]. Briefly, exponentially growing U937 or L1210 cells (1.5×10^5 cells/ml) were incubated in 96-well microtiter plates with medium containing 5, 25, 100 and 250 nM HEAMQ or combination of HEAMQ with 1 and 2 μM cisplatin or with 25 and 100 μM temozolomide in the final volume of 200 μl. After 6, 12, 18 and 24 h drug incubation at 37°C, 50 μl of MTT (1 mg/ml PBS) was added to each well followed by 4 h incubation at 37°C. Cells were centrifuged, supernatants were discarded and pellets were dissolved in 150 μl of DMSO. OD_{540nm} was determined by Microplate reader.

Analysis of drug combinations. The MTT data were analyzed using Calcusyn program to determine the IC_{50} of each drug alone. The combination index (CI)-isobologram by Chou and Talalay [18] was used to analyze drug combinations. Variable ratios of drug concentrations were used and mutually exclusive equations were applied to determine the CIs. Each CI was calculated from the mean affected fraction at each drug ratio concentration (triplicate). CI > 1, CI = 1, and CI < 1 indicate antagonism, additive effect, or synergism, respectively.

Cell cycle measurement. U937 and L1210 cells treated with 25 and 70 nM HEAMQ for 12 and 24 h were harvested, washed in PBS, and exposed to 0.1% Triton X-100 in PBS supplemented with RNAse (50 μg/ml) for 25 min at 37°C. DNA was stained by PI (50 μg/ml) for 20 min at 4°C. Samples were analyzed by EPICS XL flow cytometry (Beckman Coulter Company, CI, USA), with the use of software provided by the manufacturer.

Detection of caspase-3 and caspase-9 activities. U937 and L1210 cell treated with 70 nM HEAMQ for 0 – 24 h were collected, washed with PBS and resuspended in lysis buffer (50 mM Tris-HCl (pH 7.4), 1 mM EDTA, 10 mM EGTA). Cell lysates were clarified by centrifugation (16.000 g, 10 min, 4°C). Cleared lysates containing 50 μg of proteins were incubated with 100 μM of enzyme-specific colorigenic substrates (Ac-DEVD-pNA for caspase-3, Ac-LEHD-pNA for caspase-9) at 37°C for 2 h. The activity of caspase-3 and caspase-9 was determined as the cleavage of the colorimetric substrate by measuring the OD_{504nm}.

Western blot analysis. U937 cells treated with 70 nM HEAMQ for 0 – 24 h were collected, washed twice with PBS and lysed in lysis buffer (25 mM Tris–HCl (pH 7.2), 0.1% SDS, 0.1% Triton X-100, 150 mM NaCl, 1 mM EDTA, protease inhibitors) for 30 min at 4°C. Supernatants were cleared by centrifugation (16.000 g, 3 min, 4°C). Proteins (50 μg) were resolved on 10% SDS-PAGE gel and transferred to PVDF membrane. Membrane was blocked and proteins were detected using corresponding primary antibodies, followed by incubation with secondary antibodies. The signal was visualized using an ECL detection kit.

Cytochrome c assay. Isolation of cytosolic and mitochondrial fractions was performed according to the Cytochrome *c* ELISA Kit protocol (MBL International Corporation). Briefly, about 5 x 10^6 U937 cells treated with 25 and 70 nM HEAMQ for 12 h were collected, washed with PBS and homogenized in a homogenizing buffer. Homogenates were centrifuged (10.000 g, 30 min, 4°C) and supernatants were collected and used as cytosolic fractions. Pellets were resuspended in ice cold buffer-2 and sonicated for three times (20 sec, 4°C). Homogenates were centrifuged (10.000 g, 15 min, 4°C) and supernatants were collected and used as mitochondria fractions. Cytosolic and mitochondrial fractions were assayed separately for cytochrome *c* using the Cytochrome *c* ELISA kit by measuring the OD_{450nm}.

MAPK inhibitor treatment. To investigate the effect of MAPK inhibitors on HEAMQ-induced cell cycle arrest and apoptosis, cells were preincubated for 2 h with 20 μM SP600125 (JNK inhibitor), 20 μM SB203580 (p38 inhibitor) or 20 μM PD98059 (ERK inhibitor) before the addition of 70 nM HEAMQ.

Animals. Inbred DBA/2J mice of both sexes (weighing 18 – 22g) were obtained from the breeding facility of the Cancer Research Institute of SAS (Bratislava, Slovakia). The animals were reared under standard conditions. Food and water were provided *ad libitum*. All experiments were performed in full adherence with the European Community Guidelines principles for the care and use of laboratory animals.

In vivo experiment. L1210-leukemia bearing mice were used as antileukemic model of therapy [19]. The experimental animals were intraperitoneally implanted with L1210 leukemia cells (1 x 10^5 cells per mouse). The chemotherapy was started 1 day later as a single dose of 2.5 mg/kg of cisplatin, 15 mg/kg of temozolomide, 4 mg/kg of HEAMQ and combination of 2.5 mg/kg of cisplatin with 4 mg/kg of HEAMQ or 15 mg/kg of temozolomide and 4 mg/kg of HEAMQ. The drugs were administered intraperitoneally (0.5 ml per mouse). Animals were observed daily for the development of ascites and leukemia related death. Mean survival time (MST) and percentage of increase of life span (% ILS) were calculated and compared with MST of untreated control group.

Statistics. The data are expressed as the means ± SD of three independent experiments. The median and standard deviation were calculated using Excel software (Microsoft Office). The statistical significance of the results obtained was evaluated by a Student´s *t*-test, with probability values of $P < 0.05$ and $P < 0.001$ being considered as significant or highly significant, respectively.

Results

Effect of HEAMQ on cell viability. To check the effect of HEAMQ on cell growth, U937 and L1210 cells were treated with increasing concentrations of HEAMQ for 0 – 24 h, and cell viability was assessed by MTT assay. As presented in Figure 1, viability of U937 and L1210 cells decreased in a dose- and time-dependent manner with an IC_{50} values of 68.5 nM for U937 and of 60.2 nM for L1210 cells at 24 h treatment.

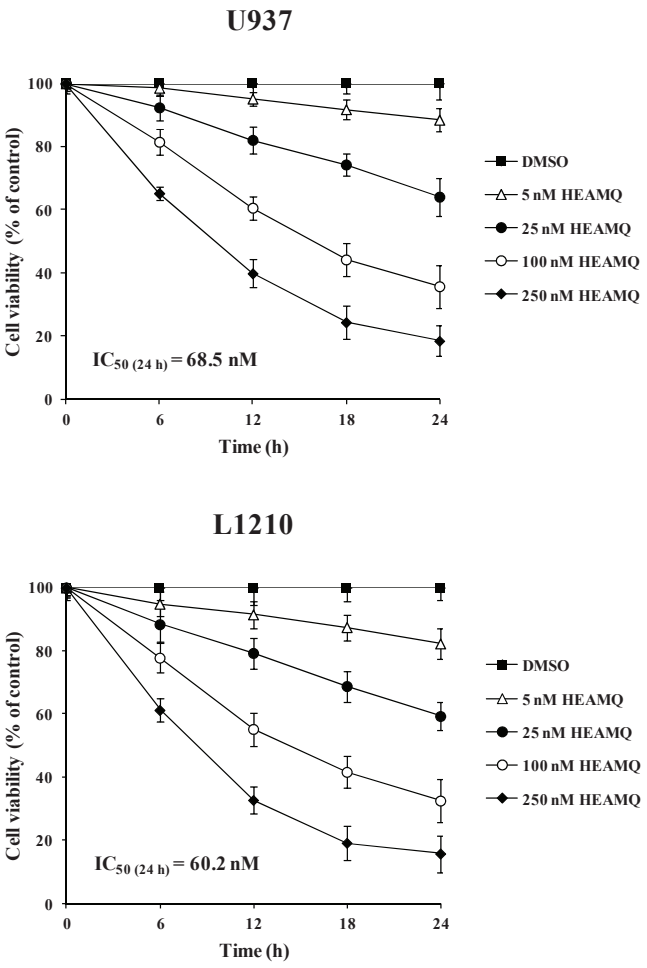

Figure 1. Effect of HEAMQ on viability of U937 and L1210 cells. Cells were treated with HEAMQ at the indicated concentrations for indicated time. Cell viability was performed using MTT assay as described in Materials and Methods. The graphs display the mean ± SD of the three independent experiments.

Effect of HEAMQ on cell cycle. To investigate the mechanisms associated with HEAMQ-induced inhibition of cell proliferation, the effects of HEAMQ treatment on cell cycle profile of U937 and L1210 cells was examined. As presented in Table 1, cells treated with HEAMQ were significantly accumulated in the G_2/M phase of the cell cycle. 70 nM HEAMQ treatment for 24 h increased the percentage of cells in the G_2/M phase from 17.9% to 57.8% for U937 and from 11.6% to 48.2% for L1210 cells, with a parallel reduction in the percentage of cells in G_0/G_1 and S phases. These results suggested that HEAMQ inhibits cell proliferation through the G_2/M phase arrest of the cell cycle.

Induction of apoptosis by HEAMQ. To determine whether HEAMQ induces cell death through apoptotic pathway, the

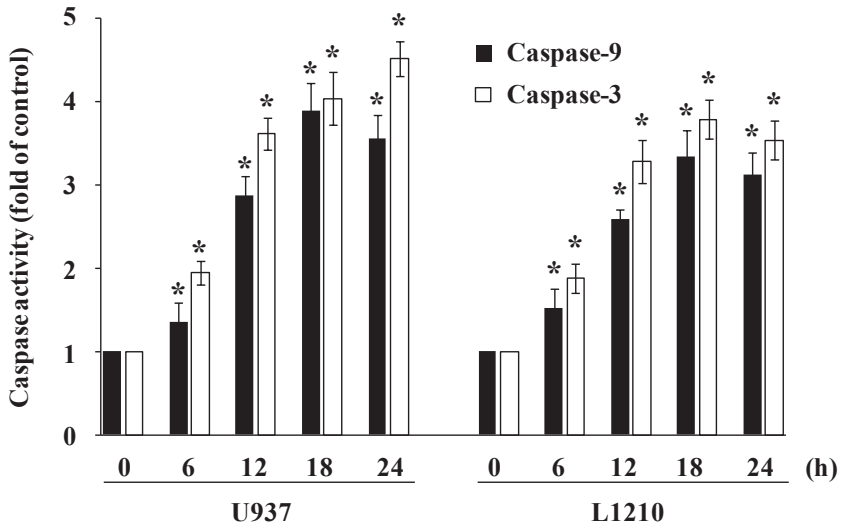

Figure 2. Effects of HEAMQ on caspase activation. Cells were treated with 70 nM of HEAMQ for indicated time. Cell lysates were prepared and enzymatic activities of caspase-3 and caspase-9 proteases were determined by incubation of 50 µg/ml total proteins with colorigenic substrates for 2 h at 37°C. The release of pNA was monitored by measuring the OD_{504nm}. Data are plotted as the mean ± SD derived from three independent experiments. * P < 0.05.

content of sub-G_0 DNA in HEAMQ-treated cells was analyzed by flow cytometry. As presented in Table 1, HEAMQ treatment resulted in a marked increase in accumulation of cells in sub-G_0 phase in a dose- and time-dependent manner (1.4% *vs.* 13.9% and 35.6% for U937 cells and 0.9% *vs.* 15.3% and 32.4% for L1210 cells treated for 24 h with 25 and 70 nM HEAMQ, respectively). In addition, a marked increase in the activity of both caspase-9 and caspase-3 was detected in cells treated with 70 nM HEAMQ (Figure 2) in the fashion coinciding with sub-G_0 peaks (Table 1). Taken together, we conclude that HEAMQ is a potent inducer of apoptosis of U937 and L1210 cells.

Effect of HEAMQ on the expression of cell cycle regulating proteins. To evaluate the role of the cell cycle regulating proteins in the G_2/M phase arrest induced by HEAMQ, protein extracts were prepared from U937 cells treated with 70 nM HEAMQ for 0 – 24 h. As shown in Figure 3, HEAMQ treatment time-dependently caused a marked decrease in cyclin A, cyclin B, and Cdk1 expression, whereas the expression of Cdk2 was unaltered. These results suggested that HEAMQ induces G_2/M arrest by altering the G_2/M cell cycle regulation protein expression in U937 cells.

Effect of HEAMQ on the expression levels of Bcl-2 and IAPs family proteins. To analyze HEAMQ-induced changes in expression of proteins that regulate apoptotic pathway, the protein extracts prepared from HEAMQ-treated U937 cells were analyzed. As shown in Figure 4, the exposure of cells to

Table 1. Cell cycle profiles of U937 and L1210 cells treated with indicated concentrations of HEAMQ for 12 and 24 h. Data represent the mean ± SD derived from three independent experiments.

Cells	Exposure (h)	HEAMQ (nM)	Cell cycle phase (%)			
			sub-G_0	G_0/G_1	S	G_2/M
U937	12	-	1.6 ± 0.4	38.9 ± 2.8	43.8 ± 3.1	17.3 ± 1.2
		25	6.4 ± 1.1	34.6 ± 1.9	38.5 ± 2.8	26.9 ± 2.7
		70	17.3 ± 2.9	30.9 ± 2.4	31.9 ± 2.2	37.4 ± 3.6
	24	-	1.4 ± 0.3	37.8 ± 1.9	44.3 ± 2.7	17.9 ± 1.5
		25	13.9 ± 2.4	33.4 ± 2.3	31.2 ± 2.4	35.4 ± 2.9
		70	35.6 ± 2.7	17.1 ± 2.7	25.1 ± 3.8	57.8 ± 3.2
L1210	12	-	1.2 ± 0.6	41.3 ± 2.9	47.8 ± 1.3	10.9 ± 1.4
		25	5.7 ± 1.9	36.1 ± 2.2	42.1 ± 3.2	21.8 ± 3.7
		70	19.2 ± 2.4	34.6 ± 3.1	35.7 ± 2.9	29.7 ± 2.6
	24	-	0.9 ± 0.3	42.1 ± 1.9	46.3 ± 2.8	11.6 ± 1.5
		25	15.3 ± 2.8	32.1 ± 2.6	35.6 ± 3.1	32.3 ± 3.1
		70	32.4 ± 3.1	22.9 ± 3.3	28.9 ± 3.2	48.2 ± 3.9

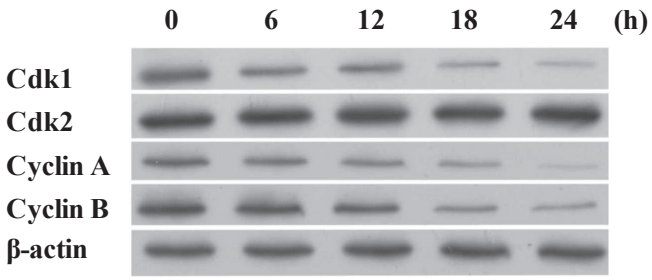

Figure 3. Immunoblot analysis for the levels of cell cycle regulatory proteins. Cells were treated with 70 nM of HEAMQ for indicated time. Total cell lysates were prepared and 50 μg of protein was subjected to SDS-PAGE followed by Western blot analysis. Each antigenic protein was detected by using the respective antibody against Cdk1, Cdk2, cyclin A, cyclin B or β-actin.

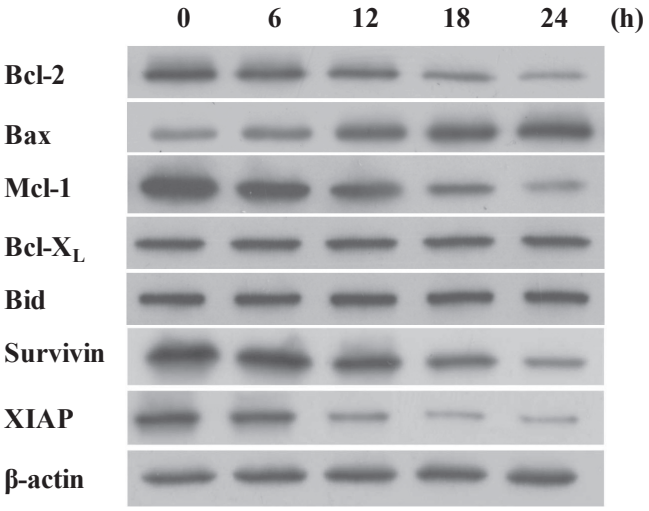

Figure 4. Western blot analysis of modulation of Bcl-2 family proteins and expression of XIAP and survivin. Cells were treated with 70 nM of HEAMQ for indicated time. Total cell lysates were prepared and 50 μg of protein was subjected to SDS-PAGE followed by Western blot analysis. Each antigenic protein was detected by using the respective antibody against Bcl-2, Bax, Mcl-1, Bcl-X_L, Bid, survivin, XIAP or β-actin.

70 nM HEAMQ for 0 – 24 h resulted in down-regulation of Bcl-2 and Mcl-1 expression, while Bax expression was notably up-regulated. Alternatively, the level of Bcl-X_L and Bid proteins were unaltered. In addition to Bcl-2 family proteins, the IAP family proteins regulate apoptotic signaling cascade by blocking caspase activities [20]. The expression of two members of IAP family proteins, survivin and XIAP, were examined in HEAMQ-treated cells. As presented in Figure 4, treatment of U937 cells with HEAMQ resulted in reducing protein expression of survivin and XIAP.

HEAMQ induces apoptosis by mitochondrial pathway. Mitochondria play a critical role in apoptosis by modulating Bcl-2 family members, such as Bcl-2, Mcl-1 and Bax, and releasing apoptogenic factors, such as cytochrome *c* [4]. As shown in Figure 4, HEAMQ treatment elicited an increase in Bax expression and a decrease in Bcl-2 and Mcl-1 expression in U937 cells. Consistent with these results, increase in cytochrome *c* release into cytosol was noted after exposure of U937 cells to HEAMQ (Figure 5). These results suggested that HEAMQ-induced apoptosis is mediated through a mitochondria-dependent pathway.

Effect of MAPK inhibitors on HEAMQ-induced G_2/M phase arrest and apoptosis. To demonstrate that MAPK pathways are involved in mediating the HEAMQ-induced apoptosis and G_2/M phase arrest, the effects of three highly specific MAPK inhibitors, namely SB203580 (p38 inhibitor), SP600125 (JNK inhibitor) and PD98059 (ERK inhibitor) on the cytotoxic effect of HEAMQ were evaluated. As shown in Table 2, HEAMQ-induced apoptosis and cell cycle arrest were markedly attenuated by pretreatment of cells with SP600125 and SB203580. However, HEAMQ-induced apoptosis and G_2/M phase arrest were not affected by ERK inhibitor (PD98059) pretreatment. These results revealed that HEAMQ-induced apoptosis and cell cycle arrest are related to JNK/p38 MAPK signaling pathway in U937 and L1210 cells. To further elucidate whether the pathways of JNK and p38 MAPK are involved in downstream molecular events of apoptosis,

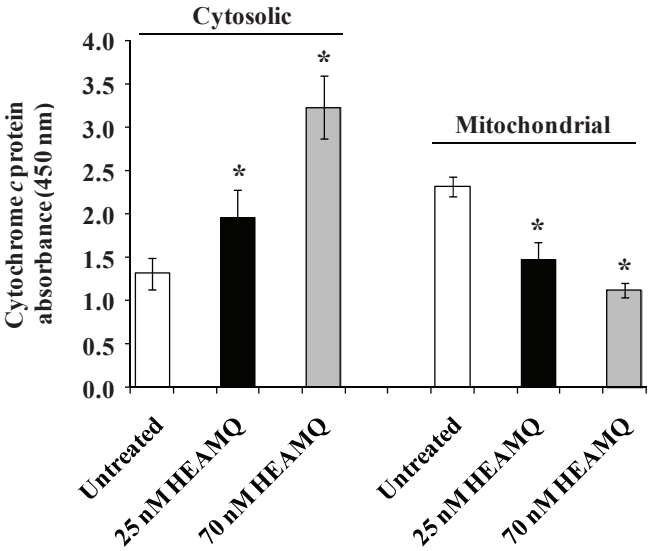

Figure 5. Release of cytochrome *c* from mitochondria. Cells were treated with 25 or 70 nM of HEAMQ for 12 h. Cytosolic and mitochondrial fractions were prepared and assayed as described in Materials and Methods section. The data are the mean ± SD derived from three independent experiments. * $P < 0.05$.

U937 cells were pretreated with SP600215 and SB203580 for 2 h, and then incubated with HEAMQ for another 24 h. As shown in Figure 6, both inhibitors blocked HEAMQ-induced up-regulation of Bax. Likewise, HEAMQ-induced down-regulation of Bcl-2, survivin and XIAP was markedly abrogated by SP600215 and SB203580. These biochemical

Table 2. Cell cycle profiles of U937 and L1210 cells pretreated for 2 h with 20 μM MAPK inhibitors, followed by treatment with HEAMQ for another 24 h. Data represent the mean ± SD derived from three independent experiments.

Cells	HEAMQ (nM)	MAPK inhibitor	Cell cycle phase (%)			
			sub-G_0	G_0/G_1	S	G_2/M
U937	-	-	1.4 ± 0.3	37.8 ± 1.9	44.3 ± 2.7	17.9 ± 1.5
	70	-	35.6 ± 2.7	17.1 ± 2.7	25.1 ± 3.8	57.8 ± 3.2
	70	SP600125*	8.9 ± 0.8	31.8 ± 2.4	39.9 ± 3.2	28.3 ± 4.7
	70	SB203580*	6.3 ± 1.4	34.4 ± 2.6	42.7 ± 2.5	22.9 ± 2.8
	70	PD98059*	33.9 ± 4.1	19.4 ± 2.2	24.7 ± 2.9	55.9 ± 3.6
L1210	-	-	0.9 ± 0.3	42.1 ± 1.9	46.3 ± 2.8	11.6 ± 1.5
	70	-	32.4 ± 3.1	22.9 ± 3.3	28.9 ± 3.2	48.2 ± 3.9
	70	SP600125*	4.1 ± 1.2	39.9 ± 2.8	42.3 ± 1.8	17.8 ± 3.9
	70	SB203580*	5.2 ± 2.3	40.3 ± 1.9	44.9 ± 3.8	14.8 ± 2.7
	70	PD98059*	27.8 ± 2.9	25.1 ± 2.7	29.8 ± 2.2	45.1 ± 3.7

*Note: SP600125 (JNK inhibitor); SB203580 (p38 inhibitor); PD98059 (ERK inhibitor).

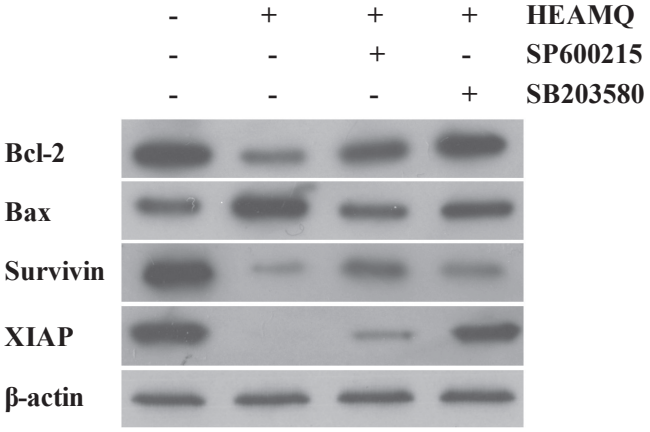

Figure 6. Western blot analysis of expression levels of Bcl-2, Bax, survivin, XIAP and β-actin. Cells were preincubated for 2 h with 20 μM SP600125 (JNK inhibitor) or 20 μM SB203580 (p38 inhibitor) followed by incubation with 70 nM HEAMQ for another 24 h. Each antigenic protein was detected by using the respective antibody.

Table 3. Effect of combinations of HEAMQ and cisplatin or temozolomide on viability of U937 and L1210 cells after 24 h application. Data represent the mean derived from three independent experiments.

Drug combinations		Combination index (CI) [a]	
		U937	L1210
1 μM cisplatin	+ 5 nM HEAMQ	0.874	0.839
	+ 25 nM HEAMQ	0.524	0.658
2 μM cisplatin	+ 5 nM HEAMQ	0.639	0.743
	+ 25 nM HEAMQ	0.421	0.436
25 μM temozolomide	+ 5 nM HEAMQ	0.925	0.912
	+ 25 nM HEAMQ	0.738	0.619
100 μM temozolomide	+ 5 nM HEAMQ	0.743	0.729
	+ 25 nM HEAMQ	0.527	0.488

[a] CI was calculated as described in Materials and Methods section. Antagonism (CI>1); Synergism (CI<1).

changes reinforced the fact that HEAMQ-induced apoptosis is mediated through activation of JNK and p38 MAPK. Taken together, JNK and p38 MAPK activation plays a vital role in HEAMQ-induced apoptosis and G_2/M cell cycle phase arrest in U937 cells.

Effect of HEAMQ on therapeutic efficacies of cisplatin and temozolomide. To reveal full therapeutic potential of HEAMQ for combination chemotherapy, ability of HEAMQ to modulate therapeutic efficacies of cisplatin and temozolomide was tested. As presented in Table 3, HEAMQ increased the efficacy of both chemotherapeutics. Drug combination studies by MTT test demonstrated that HEAMQ combined with cisplatin or temozolomide synergistically enhanced their antiproliferative activities (CI<1).

In vivo experiment. To check the therapeutic efficacy of HEAMQ under *in vivo* conditions, combination chemotherapy of HEAMQ with cisplatin or temozolomide was tested using L1210-leukemia bearing mice. As showed in Figure 7 and Table 4, the synergistic action of HEAMQ was registered for its combination with cisplatin or temozolomide, respectively. This resulted in significant increase in life span for combinations of HEAMQ with cisplatin (85.7%) or HEAMQ with temozolomide (92.9%) compared to single treatment of L1210-leukemia bearing mice with cisplatin (29.8%), temozolomide (22.6%) or HEAMQ (33.3%).

Discussion

Successful treatment of leukemia cells with chemotherapeutic agents largely depends on their ability to induce cell cycle arrest and apoptosis. Therefore, novel inducers of apoptosis provide a new therapeutic approach for antineoplastic treatment. Several Cdks regulate the cell cycle progression in mammalian cells [2]. Among the Cdks that regulate cell cycle progression, Cdk1 and Cdk2 kinases are activated in association with cyclins A and B during the G_2/M phase transition.

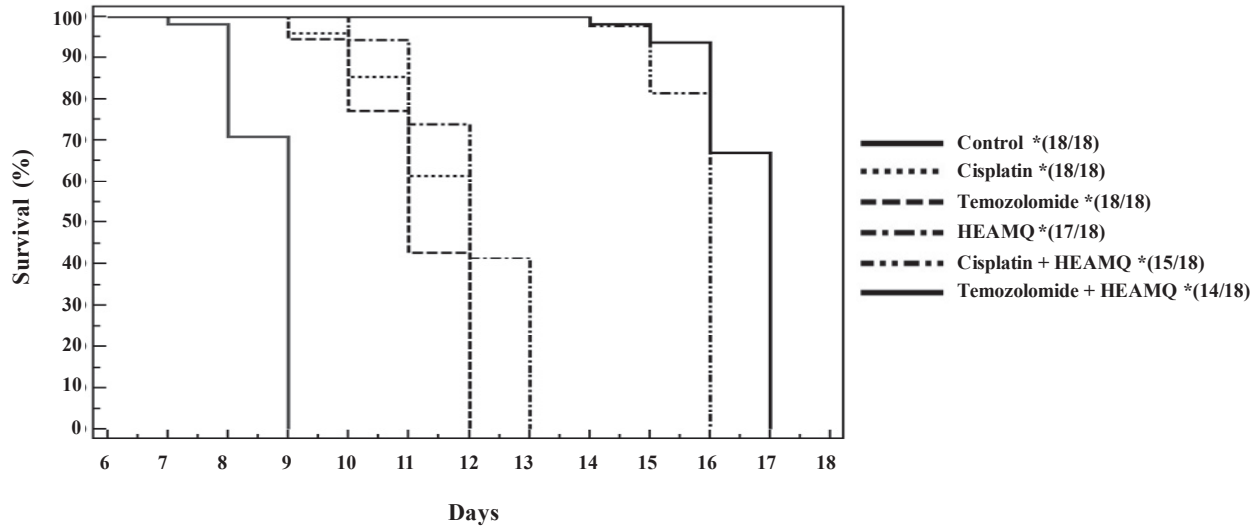

Figure 7. Mice survival curve. DBA/2J mice of both genders intraperitoneally implanted with 1 x 10^5 L1210 cells per mouse were treated with a single dose of 2.5 mg/kg of cisplatin, 15 mg/kg of temozolomide, 4 mg/kg of HEAMQ and combination of 2.5 mg/kg of cisplatin with 4 mg/kg of HEAMQ or 15 mg/kg of temozolomide and 4 mg/kg of HEAMQ as described in Materials and Methods section. * – Number of leukemia related death of animals *vs.* number of animals used in the study.

In this study, we showed that novel quinazolinone-based nonclassical antifolate, HEAMQ, abrogates progression of cells in G_2/M phase (Table 1) through decreasing expression of Cdk1, cyclin A and cyclin B (Figure 3). These data suggest that cell cycle arrest induced by HEAMQ is mediated by limiting the supply of Cdk1, cyclin A and cyclin B, which are essential executors in regulating transition into mitosis. Thus, it is plausible that alterations in cell cycle associated proteins lead to block at G_2/M phase in HEAMQ-treated leukemia cells.

Apoptosis is tightly regulated process under control of several signaling pathways, such as caspase and mitochondrial pathways [3-5,9,20]. In our study, HEAMQ treatment caused activation of caspase-9 and caspase-3 in a time-dependent manner (Figure 2), that was consistent with accumulation of cells in the sub-G_0 phase (Table 1). Moreover, a time-dependent increase in cytosolic cytochrome *c* was detected in HEAMQ-treated cells (Figure 5). Bcl-2 family proteins, including the anti-apoptotic Bcl-2, Bcl-X_L and Mcl-1, and the pro-apoptotic Bad, Bid and Bax proteins have been reported to regulate cytochrome *c* release from mitochondria [4,5]. It has been reported that proto-oncogene Bcl-2, which encodes an inner mitochondrial protein, is antagonizing apoptosis and its decreased expression or changes in post-transcriptional regulation might contribute to the drug-mediated lethality [5,21]. On the contrary, overexpression of Bax accelerates apoptosis induced by different stress stimuli in many cell lines [22,23]. Consistent with these observations, down-regulation of Bcl-2 and Mcl-1, increase in expression of Bax, and release of cytochrome *c* were noted with HEAMQ-treated leukemia cells (Figure 4 and Figure 5). IAPs have been reported to inhibit apoptosis via their function in inhibition of caspase-3 and caspase-7 activation. IAPs are also able to abrogate cytochrome *c*-induced activation of caspase-9 [3,5]. Our data

Table 4. Therapeutic efficacy of HEAMQ, cisplatin, temozolomide and their combinations in L1210-leukemia bearing DBA/2J mice.

Drugs	Dose# (mg/kg) *vs.* no. of animals)	Leukemia-related death (No. of death	MST (days ± SD)	ILS (%)
Control		18(18)	8.4 ± 1.2	0
Cisplatin	2.5	18(18)	10.9 ± 2.3	29.8*
Temozolomide	15	18(18)	10.3 ± 1.7	22.6*
HEAMQ	4	17(18)	11.2 ± 2.1	33.3*
Cisplatin + HEAMQ	2.5 + 4	15(18)	15.6 ± 1.3	85.7**
Temozolomide + HEAMQ	15 + 4	14(18)	16.2 ± 2.4	92.9**

Note: # – Drugs were administered intraperitoneally as a single dose 1 day after intraperitoneal implantation of 1 x 10^5 L1210 cell per mouse (see Materials and Methods section).

MST – mean survival time, ILS – increase of life span, *P < 0.05, **P < 0.001.

reveal that the protein expression of XIAP and survivin was decreased by HEAMQ treatment (Figure 4). Taken together, our results clearly demonstrated that dysregulation of Bcl-2 family members by HEAMQ treatment led to mitochondrial-dependent apoptotic death of U937 cells.

Recent evidence indicates that the MAPK family proteins are important mediators of apoptosis induced by stress stimuli [6,7]. JNK signaling pathway has been reported to affect the members of the Bcl-2 family by eliciting mitochondrial translocation of Bax [8]. Importantly, p38 MAPK regulates the ratio of Bax and anti-apoptotic members, whose dysregulation is leading to an increase in mitochondrial membrane permeability, the release of cytochrome *c*, and activation of caspases [9]. In the present study, HEAMQ-induced Bcl-2, XIAP and survivin down-regulation and Bax up-regulation were abolished by pretreatment with JNK-specific inhibitor SP600125 and p38 kinase-specific inhibitor SB203580 (Figure 6). These data suggest that JNK and p38 MAPK pathways are involved in HEAMQ-induced apoptosis in leukemia cells.

Since many chemotherapeutic drugs used for treatment of tumors could enhance or diminish action of other active agents and *in vivo* effectiveness of combination treatment is extremely important for development of new chemotherapy agents [24,25], combination chemotherapy of HEAMQ with cisplatin and temozolomide under *in vitro* and *in vivo* conditions was tested. Results of MTT study showed that HEAMQ significantly enhanced therapeutic efficacy when used in combination with cisplatin or temozolomide (Table 3). This effect probably involves activation of apoptosis by HEAMQ through alteration of anti-apoptotic and pro-apoptotic proteins making thus leukemia cells more sensitive to chemotherapeutic drugs. Although the exact mechanism of synergy of cisplatin and HEAMQ is not fully understood, there is accumulating evidence of a key role for p38 MAPK pathway activation in the cellular response to cisplatin. Additionally, it has been postulated that prolonged activation of JNK pathway is sensitizing cells to cisplatin [26]. As HEAMQ-induced apoptosis features are blocked by pretreatment of cells with JNK and p38 inhibitors (Figure 6 and Table 2), it is plausible that activating JNK and p38 MAPK pathway by HEAMQ increases sensitivity of cells to cisplatin. Interestingly, combination of HEAMQ with cisplatin or temozolomide *in vivo* followed synergistic action detected *in vitro*, and increased life span of L1210-leukemia bearing mice was observed when combinations of HEAMQ with cisplatin or temozolomide were applied, compared to single treatment regiment (Figure 7 and Table 4).

Taken together, our results clearly demonstrated that novel quinazolinone-based nonclassical antifolate, HEAMQ, possesses strong antineoplastic activity associated with G_2/M cell cycle arrest, down-regulation of cyclin-dependent protein kinases, dysregulation of Bcl-2 family members and induction of apoptosis, and highlighted that this agent could be used to further increase therapeutic efficacies of traditional chemotherapeutic agents.

Acknowledgments: This work was supported by Scientific Grant Agency of Slovak Academy of Sciences VEGA grant number 2/0004/10.

References

[1] ORREN DK, PETERSEN LN, BOHR VA. Persistent DNA damage inhibits S-phase and G2 progression, and results in apoptosis. Mol Cell Biol 1997; 8: 1129–1142.

[2] SANTAMARIA D, ORTEGA S. Cyclins and CDKS in development and cancer: lessons from genetically modified mice. Front Biosci 2006; 11: 1164–1188. http: //dx.doi.org/10.2741/1871

[3] DANSON S, DEAN E, DIVE C, RANSON M. IAPs as a target for anticancer therapy. Curr Cancer Drug Targets 2007; 7: 785–794. http: //dx.doi.org/10.2174/156800907783220471

[4] MARTINOU JC, YOULE RJ. Mitochondria in apoptosis: Bcl-2 family members and mitochondrial dynamics. Dev Cell 2011; 21: 92–101. http: //dx.doi.org/10.1016/j.devcel.2011.06.017

[5] ANTONSSON B, MARTINOU JC. The Bcl-2 protein family. Exp Cell Res 2000; 256: 50–57. http: //dx.doi.org/10.1006/excr.2000.4839

[6] DAVIS RJ. Signal transduction by the JNK group of MAP kinases. Cell 2000; 103: 239–252. http: //dx.doi.org/10.1016/S0092-8674(00)00116-1

[7] JOHNSON GL, LAPADAT R. Mitogen-activated protein kinase pathways mediated by ERK, JNK, and p38 protein kinases. Science 2002; 298: 1911–1912. http: //dx.doi.org/10.1126/science.1072682

[8] LEE HJ, WANG CJ, KUO HC, CHOU FP, JEAN LF, et al. Induction apoptosis of luteolin in human hepatoma HepG2 cells involving mitochondria translocation of Bax/Bak and activation of JNK. Toxicol Appl Pharmacol 2005; 203: 124–131. http: //dx.doi.org/10.1016/j.taap.2004.08.004

[9] MANDAL C, DUTTA A, MALLICK A, CHANDRA S, MISRA L, et al. Withaferin A induces apoptosis by activating p38 mitogen-activated protein kinase signaling cascade in leukemic cells of lymphoid and myeloid origin through mitochondrial death cascade. Apoptosis 2008; 13: 1450–1464. http: //dx.doi.org/10.1007/s10495-008-0271-0

[10] SELVAM TP, KUMAR PV. Quinazoline marketed drugs – a review. Research in Pharmacy 2011; 1: 1–21.

[11] SHARMA CP, KAUR G, PAHWA R, SHARMA A, RAJAK H. Quinazolinone analogs as potential therapeutic agents. Curr Med Chem 2011; 18: 4786-4812.

[12] CONNOLLY DJ, CUSACK D, SULLIVAN TPO, GUIRY PJ. Synthesis of quinazolinones and quinazolines. Tetrahedron 2005; 61: 10153–10202. http: //dx.doi.org/10.1016/j.tet.2005.07.010

[13] JANTOVA S, KONARIKOVA K, LETASIOVA S, PAULOVICOVA E, MILATA V, et al. Photochemical and phototoxic properties of ethyl 1,4-dihydro-8-nitro-4-oxoquinoline-3-carboxylate, a new quinoline derivative. J Photochem Photobiol B 2011; 102: 77–91. http: //dx.doi.org/10.1016/j.jphotobiol.2010.09.007

[14] JANG JS, HOUR MJ, HUANG WW, LIN KL, KUO SC, et al. MJ-29 inhibits tubulin polymerization, induces mitotic

arrest, and triggers apoptosis via cyclin-dependent kinase 1-mediated Bcl-2 phosphorylation in human leukemia U937 cells. J Pharmacol Exp Ther 2010; 334: 477–488. http: //dx.doi.org/10.1124/jpet.109.165415

[15] SPIRKOVA K, STANKOVSKY S, MRVOVA A, CIPAK L. Synthesis and biological activity of some 2-substituted quinazoline-4-ones. Chem Papers 1999; 53: 272–275.

[16] HUANG YL, LIN CF, LEE YJ, LI WW, CHAO TC, et al. Non-classical antipholates, 5-(N-phenylpyrrolidin-3-yl)-2,4,6-triaminopyrimidines and 2,4-Diamino-6(5H)-oxopyrimidines, synthesis and antitumor studies. Bioorg Med Chem 2003; 11: 145–157. http: //dx.doi.org/10.1016/S0968-0896(02)00238-9

[17] CARMICHAEL J, DEGRAFF WG, GAZDAR AF, MINNA JD, MITCHELL JB. Evaluation of tetrazolium-based semiautomated colorometric assays: assessment of chemosensitivity testing. Cancer Res 1987; 47: 936–942.

[18] CHOU TC, TALALAY P. Analysis of combined drug effects: a new look at a very old problem. Trends Pharmacol Sci 1983; 4: 450–454. http: //dx.doi.org/10.1016/0165-6147(83)90490-X

[19] FRITZER-SZEKERES M, NOVOTNY L, ROMANOVA D, GOBL R, SEDLAK J, et al. Enhanced effects of adriamycin by combination with a new ribonucleotide reductase inhibitor, trimidox, in murine leukemia. Life Sci 1998; 63: 545–552. http: //dx.doi.org/10.1016/S0024-3205(98)00305-1

[20] VERHAGEN AM, COULSON EJ, VAUX DL. Inhibitor of apoptosis proteins and their relatives: IAPs and other BIRPs. Genome Biol 2001; 2: 3009.1-3009-10.

[21] WILLIMOTT S, WAGNER SD. Post-transcriptional and post-translational regulation of Bcl-2. Biochem Soc Trans 2010; 38: 1571–1575. http: //dx.doi.org/10.1042/BST0381571

[22] FINUCANE DM, BOSSY-WETZEL E, WATERHOUSE NJ, COTTER TG, GREEN DR. Bax-induced caspase activation and apoptosis via cytochrome c release from mitochondria is inhibitable by Bcl-XL. J Biol Chem 1999; 274: 2225–2233. http: //dx.doi.org/10.1074/jbc.274.4.2225

[23] ZHENG JY, YANG GS, WANG WZ, LI J, LI KZ, et al. Over-expression of Bax induces apoptosis and enhances drug sensitivity of hepatocellular cancer-9204 cells. World J Gastroenterol 2005; 11: 3498–3503.

[24] CHOU TC. Preclinical versus clinical drug combination studies. Leuk Lymphoma 2008; 49: 2059–2080. http: //dx.doi.org/10.1080/10428190802353591

[25] FREI E, ANTMAN KH. Combination chemotherapy, dose, and schedule. In: Holland JF, Bast RC, Morton DL, Frei E, Kufe DW, Weichselbaum RR, editors. Cancer Medicine. Baltimore: Williams & Wilkins,1997: 817–837.

[26] CEPEDA V, FUERTES MA, CASTILLA J, ALONSO C, QUEVEDO C, et al. Biochemical mechanism of cisplatin cytotoxicity. Anticancer Agents Med Chem 2007; 7: 3–18. http: //dx.doi.org/10.2174/187152007779314044